Chem. Res. Chinese Universities, 2020, 36(5), 927—933 doi: 10.1007/s40242-020-0007-4

Article

Preparation of pH-Responsive Doxorubicin Nanocapsules by Combining High-gravity Antisolvent Precipitation with *In-situ* Polymerization for Intracellular Anticancer Drug Delivery

LIU Jie[1], CHEN Bo[2*] and ZHANG Jianjun[1*]

1. College of Chemical Engineering, Beijing University of Chemical Technology, Beijing 100029, P. R. China;
2. State Key Laboratory of NBC Protection for Civilian, Beijing 102205, P. R. China

Abstract Owing to the low pH value in tumor and cancer cells, drug delivery systems based on pH-responsive polymer nanocarriers have been extensively explored for anticancer chemotherapy. Herein, we developed a pH-responsive doxorubicin(DOX) nanocapsule(named as DNanoCapsule) prepared by combining *in-situ* polymerization technique with high-gravity antisolvent precipitation technique through an amphiphilic polymerized surface ligand. DNanoCapsules show an obvious spherical core-shell structure with a single DOX nanoparticle encapsulated in the polymer layer. Dissolution rate studies prove that the DNanoCapsules have robust drug-release profiles under acidic environments due to the division of the pH-sensitive cross-linker, which triggers the collapse of the polymer layer. The *in vitro* investigations demonstrated that the DNanoCapsules exhibited high cellular uptake efficiency and cytotoxicity for both HeLa and MCF-7 cancer cells. Therefore, this work may provide a promising strategy to design and develop various stimuli-responsive drug nanocapsules for the treatment of cancer or other diseases.

Keywords pH-Responsive; Nanocapsule; *In-situ* polymerization; High-gravity antisolvent precipitation; Anticancer chemotherapy

1 Introduction

Nanotechnology has revolutionized the fabrication of drug delivery systems(DDS) for the treatment of many major diseases, especially cancer[1—3]. Polymer nanocarriers with high blood circulation, tumor accumulation and penetration, cellular internalization, and stimuli-responsive drug release have been widely explored to enhance the efficacy of anticancer drugs[4—6]. As a remarkable candidate for polymer nanocarriers, the polymer nanocapsules(or nanogels) have attracted a lot of attention due to their stable structure, outstanding drug entrapment efficiency, and stimuli-responsive drug release features[7—10]. However, the therapeutic application of polymer nanocapsules is usually hampered by poor drug loading capacity(DLC) and complicated synthesis process.

In-situ surface polymerization is widely used for synthesis and surface modification of nanomaterials[11—13]. Compared with conventional synthesis method, polymer nanocapsules prepared by *in-situ* surface polymerization have variable structure design and control that could be simply manipulated by choosing various polymerization conditions and functional monomers or crosslinkers. Additionally, *in-situ* surface polymerization is a "coating from" strategy, and polymer capsule layer is grown from *in-situ* surface, resulting in avoiding the tedious separation of unconjugated polymer from the products effectively[14].

Recently, high-gravity antisolvent precipitation(HGAP) in a rotating packed bed has been utilized for preparing drug nanoparticles[15—18]. Owing to the intensified mass transfer and micromixing effect under high gravity, the drug nucleation amounts and rates can be increased greatly, leading to the formation of drug nanoparticles with a smaller size, uniform size distribution, low crystallinity, and high dissolution rate[19]. The drug nanoparticles can be modified further by introducing a surface ligand containing various active groups in HGAP, to achieve desirable functions.

Over the past several decades, a wide variety of stimuli-responsive factors have been utilized to design smart polymer nanocarriers for anticancer drug delivery[20—24]. Specifically, by taking advantage of the acidic microenvironment of tumor and cancer cells, polymer nanocarriers with acid-sensitive bonds, whose cleavage enables the rapid release of the loading drugs, have been extensively developed[25—28].

Herein, we developed a pH-responsive DOX nanocapsule(DNanoCapsule) with a high DLC *via* a simple method, in which both the HGAP and *in-situ* polymerization techniques are employed using an amphiphilic polymerized surface ligand.

*Corresponding authors. Email: zhangjj@mail.buct.edu.cn; NBC-BoChen@163.com

Received January 17, 2020; accepted February 19, 2020.

Supported by the National Natural Science Foundation of China(Nos.21476018, 21622601) and the National Key R&D Program of China(No.2015CB932101).

© Jilin University, The Editorial Department of Chemical Research in Chinese Universities and Springer-Verlag GmbH

A schematic illustration of the synthesis of the DNanoCapsule is provided in Scheme 1. Firstly, an amphiphilic polymerized acrylated-alkylphenol ethoxylate(OP-AC) was synthesized as a ligand for modifying the surface of DOX nanoparticles with acrylate groups through hydrophobic association in the HGAP process. Subsequent *in-situ* redox polymerization, using acrylamide(AAm) as the monomer, *N,N'*-methylene bisacrylamide(BIS) as the non-degradable cross-linker, and glycerol dimethacrylate(GDA) as the acidic-degradable cross-linker, resulted in both non-responsive DNanoCapsule-A and pH-responsive DNanoCapsule-B[29]. The DNanoCapsule-B can be taken by cancer cells through the endocytosis pathway and can be further degraded under the acidic microenvironment of endosomes and lysosomes to promote a robust release of the loading DOX. The releasing DOX will diffuse into the cell nucleus and intercalate on DNA to induce cell death. Moreover, investigation of the dissolution rate demonstrated that the DNanoCapsule-B exhibited a pH-responsive drug release profile. Finally, the *in vitro* cytotoxicity was evaluated against cervical carcinoma cells(HeLa) and breast carcinoma cells(MCF-7) by the MTT and live-dead assay, and the results proved that DNanoCapsule-B could induce the death of both cancer cells effectively.

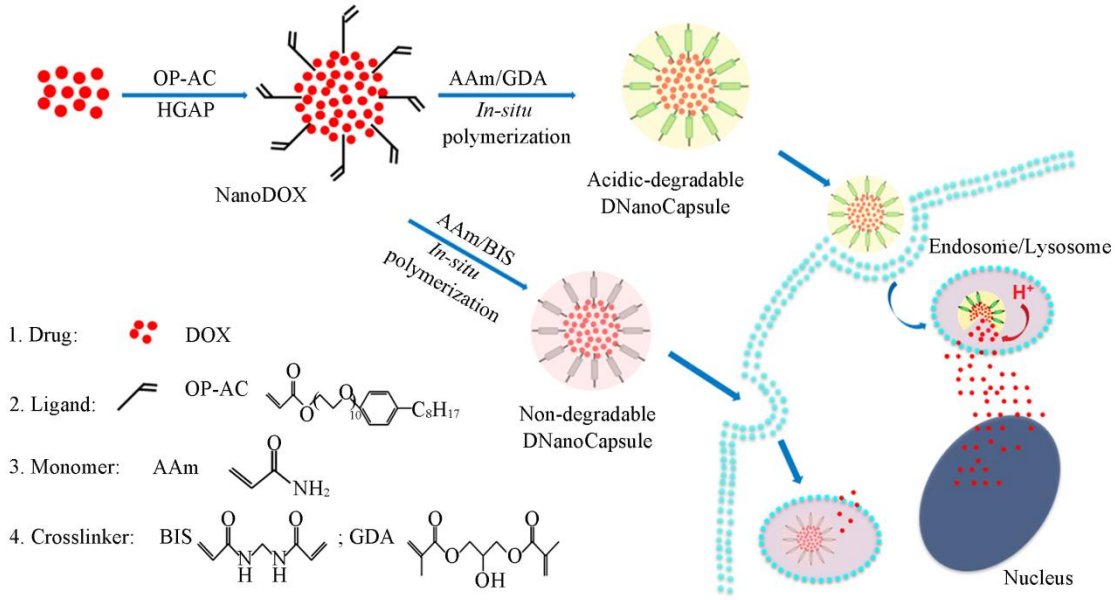

Scheme 1 Schematic illustration showing the preparation and cellular uptake of DNanoCapsules

2 Experimental

2.1 Materials

Doxorubicin hydrochloride(DOX·HCl) was purchased from Beijing ZHONGSHUO Medical Technology Development Co., Ltd., China. Breast carcinoma cells(MCF-7) and cervical carcinoma cells(HeLa) were obtained from American Type Culture Collection(ATCC). Fetal bovine serum(FBS), penicillin-streptomycin solution(100×), and DMEM cell culture medium were purchased from HyClone(Beijing, China). All other reagents were purchased from Sigma-Aldrich unless otherwise noted.

2.2 Synthesis of OP-AC

The synthesis of OP-AC is outlined in Scheme 2. Specifically, 0.033 mol of OP-10, 0.04 mol of triethylamine(TEA), and 40 mL of tetrahydrofuran(THF) were added to a three-neck flask with vigorous stirring in an ice-water bath. After mixing, 0.04 mol of methacryloyl chloride(MAC) in 10 mL of THF was added dropwise, and the reaction was carried out for another 5 h. Then, the reaction solution was removed by a rotary evaporator, and further extracted by the addition of 80 mL of acetone. Then, the mixture was centrifuged at 9000 r/min to remove the TEA hydrochloride, and the supernatant, containing OP-AC, was evaporated to obtain the final products. The OP-AC samples were characterized by ^{1}H NMR(Bruker AVANCE III HD 400 MHz NMR spectrometer), and FTIR(Bruker 70 V infrared spectrometer).

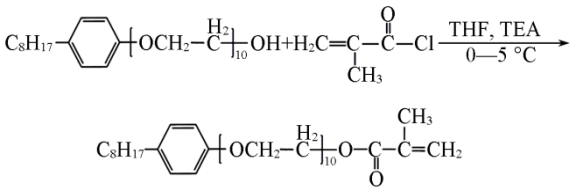

Scheme 2 Schematic illustration showing the synthesis of OP-AC

2.3 Preparation of the DNanoCapsules

Firstly, OP-AC-modified DOX nanoparticles were prepared *via* HGAP. Briefly, the DOX-base DMSO solution(10 mg/mL) and OP-AC ultrapure water solution(0.1 mg/mL) were continuously pumped from their storage reservoirs into different pipelines of the rotating packed bed(RPB) with a flow rate of 1:25 and a rotating speed of 2180 r/min. After entering the RPB, the final product of DOX/OP-AC nanoparticles was collected and dialyzed by a PBS buffer(pH 8.0, 15 mmol/L) to

remove the free DOX, OP-AC, and DMSO solvent.

Further, 20 mL of the DOX/OP-AC nanoparticle solution(DOX concentration of 0.2 mg/mL) was mixed with a certain amount of AAm monomers, and BIS or GDA cross-linkers, and the molar ratio of the monomer to cross-linker was set at 5:2. Subsequently, 200 μL of ammonium persulfate(APS, 100 mg/mL, dissolved in deionized water) and 34 μL of *N,N,N′,N′*-tetramethylethylenediamine(TEMED) was continuously added to the mixture solution to initiate the *in-situ* polymerization on the surface the of the DOX/OP-AC nanoparticles to synthesize DNanoCapsules. Finally, after dialysis and lyophilization, the DNanoCapsules powder was stored at 4 °C for further use.

The particle size and morphology of the DOX/OP-AC nanoparticles and DNanoCapsules were measured by means of dynamic light scattering(DLS, Malvern Zetasizer Nano ZS90 instrument, Malvern, UK) and transmission electron microscopy(TEM, HT7700, Hitachi, Japan).

The DOX content of the DNanoCapsules was determined by ultraviolet-visible(UV-Vis) spectrophotometry(Varian Cary 50, USA) with an absorption wavelength at 488 nm, according to the standard curve. The DOX loading capacity(LC) was calculated according to the following equation:

$$\mathrm{LC}(\%)=\frac{m_{\mathrm{L}}}{m_{\mathrm{N}}}\times 100\% \quad (1)$$

where m_{L} is the mass of the encapsulated DOX, and m_{N} is the mass of DNanoCapsules.

2.4 *In vitro* DOX Release from DNanoCapsules

The *in vitro* release behavior of DOX from the DNanoCapsules was evaluated under various pH value conditions. For this, 2 mg of DNanoCapsules were dispersed in 5 mL of the PBS buffer of various pH values(7.4, 6.0 and 5.0), and then transferred into a dialysis bag(MWCO=3500), which was immersed into 20 mL of the same pH value buffer with stirring at 37 °C. Then, 3 mL of the external buffer was taken out and replaced with the same volume of fresh medium immediately at predetermined time points. To determine the release amount of DOX, the concentration of DOX was calculated according to the standard curve by measuring the absorbance value of DOX using UV-Vis spectrophotometry at 488 nm.

2.5 *In vitro* Cellular Uptake of DNanoCapsules

The MCF-7 cell-line was obtained from American Type Culture Collection(ATCC), and the cellular uptake of the DNanoCapsules was assessed *via* confocal laser scanning microscopy(CLSM, LEICA, TCS-SP5, Germany) and flow cytometry(FCM, Beckman Coulter MoFloXDP). For CLSM imaging, MCF-7 cells were seeded in Lab-Tek chambered cover glass systems(8 wells), at a density of 8000 cells/well, in 200 μL of complete DMEM medium, and cultured overnight at 37 °C in 5% CO_2 atmosphere before use. Afterwards, the cells were incubated with 50 μL of DNanoCapsules(final DOX concentration of 10 μg/mL) for 4 h at 37 °C. After incubation, the cells were washed three times with PBS, and the cell nucleus were further stained with 4′,6-diamidino-2-phenylindole (DAPI); the extent of internalization of the DNanoCapsules was visualized using a CLSM. For FCM analysis, 100000 cells in 2 mL of medium were plated per well in a 6-well plate and cultured overnight. After adding 500 μL of DNanoCapsules for 4 h, the cells were washed three times with PBS, trypsinized, centrifuged, re-suspended in PBS, and analyzed using FCM. A total of 10000 events was analyzed per sample.

2.6 Intracellular Trafficking of DNanoCapsules

MCF-7 cells were seeded in Lab-Tek chambered coverglass systems(8 wells), at a density of 7000 cells/well, in 200 μL of complete DMEM medium, and cultured overnight at 37 °C in 5% CO_2 atmosphere before use. Further, the cells were incubated with 50 μL of DNanoCapsule solution(DOX concentration of 3 μg/mL) for 4 and 24 h at 37 °C. After incubation, the cells were stained with 50 μL of LysoTracker Green(50 nmol/L) for 2 h, and further visualized using a CLSM.

2.7 *In vitro* MTT Assay

The *in vitro* cytotoxicity of free DOX and DNanoCapsules against both HeLa and MCF-7 cell-lines was evaluated by the MTT assay. Briefly, cells were seeded in 96-well plates with a density of 4×10^3 cells/well in a 200 μL of complete DMEM medium. After incubation for 12 h, the cells were treated with free DOX and DNanoCapsules, respectively, at a DOX concentration ranging from 3.3 μg/mL to 33.3 μg/mL for 24 h. Thereafter, the supernatant was removed carefully and replaced by 100 μL of fresh complete DMEM medium. Then, 20 μL of MTT solution(5 mg/mL) was added to each well and incubated for another 4 h. Finally, the cell media were substituted with 100 μL of DMSO. The absorbance(A) of the solution was detected using a microplate reader(Thermo Fisher, MK3, America) at a wavelength of 570 nm. Cell viability was assessed *via* the formula:

$$\text{Cell viability}(\%)=A_{\text{sample}}/A_{\text{control}}\times 100\% \quad (2)$$

2.8 *In vitro* Live-dead Assay

HeLa and MCF-7 cells were seeded in Lab-Tek chambered cover glass systems(8 wells), at a density of 8000 cells/well, in 200 μL of complete DMEM medium and cultured overnight at 37 °C in 5% CO_2 atmosphere before use. Afterwards, the cells were incubated with 50 μL of free DOX and DNanoCapsules(final DOX concentration of 20 μg/mL) for 24 h at 37 °C. After incubation, the cells were washed three times with PBS and further stained with a live-dead viability/cytotoxicity kit(Molecular Probes, Eugene, OR) using the manufacturer's protocol. Each sample was stained with 100 μL of the staining solution for 30 min at 37 °C in a dark environment and imaged with a CLSM.

2.9 Statistical Analysis

All statistical analyses were performed using Instat(GraphPad, San Diego, CA) and SPSS 20.0(Chicago, USA). Experiments were statistically analyzed using the one-way

ANOVA test to compare all pairs of data using a 95% confidence interval.

3 Results and Discussion

3.1 Preparation and Characterization of DNanoCapsules

An OP-AC amphiphilic polymerized surface ligand was synthesized by modifying OP-10 with methacryloyl chloride[30]. Fig.1(A) shows the ^{1}H NMR spectra of OP-10 and OP-AC with proton peaks at δ 5.5 and 6.5, attributed to the carbon-carbon double bond(—C═C—) of acrylate groups[31]. The FTIR spectra of OP-10 and OP-AC are shown in Fig.1(B). Compared to that of OP-10, the hydroxyl stretching vibration(3460 cm^{-1}) of OP-10 almost disappeared, and the carbonyl and —C═C— stretching vibration of acrylate appeared at 1731 and 1617 cm^{-1}, thus suggesting that OP-10 was successfully modified by acrylate groups.

Furthermore, the OP-AC-modified DOX nanoparticles were prepared *via* HGAP. An average size of around 68 nm was determined by DLS measurement[Fig.1(C)]. The TEM image shows that the DOX nanoparticles were spherical with a particle size in the range of 50—100 nm[Fig.1(D)].

In-situ polymerization was initiated on the surface of the OP-AC-modified DOX nanoparticles by incorporating BIS or GDA cross-linkers to obtain the DNanoCapsules. As shown in Fig.2(A) and (B), the average sizes of DNanoCapsule-A and DNanoCapsule-B were determined to be around 266.8 nm

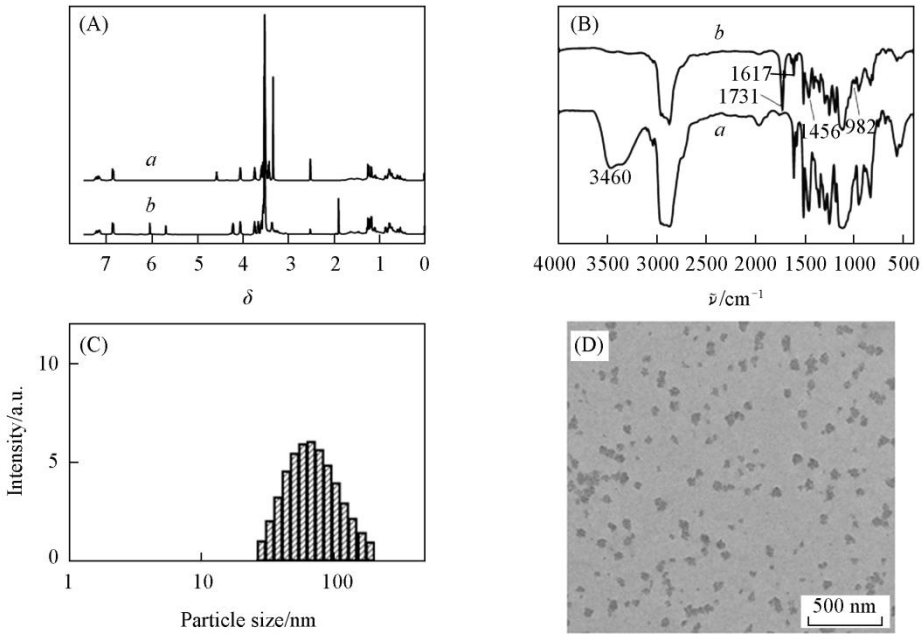

Fig.1 ^{1}H NMR spectra(A) and FTIR spectra(B) of OP-10(*a*) and OP-AC(*b*), particle size distribution of DOX nanoparticles determined by DLS(C) and TEM image of DOX nanoparticles(D)

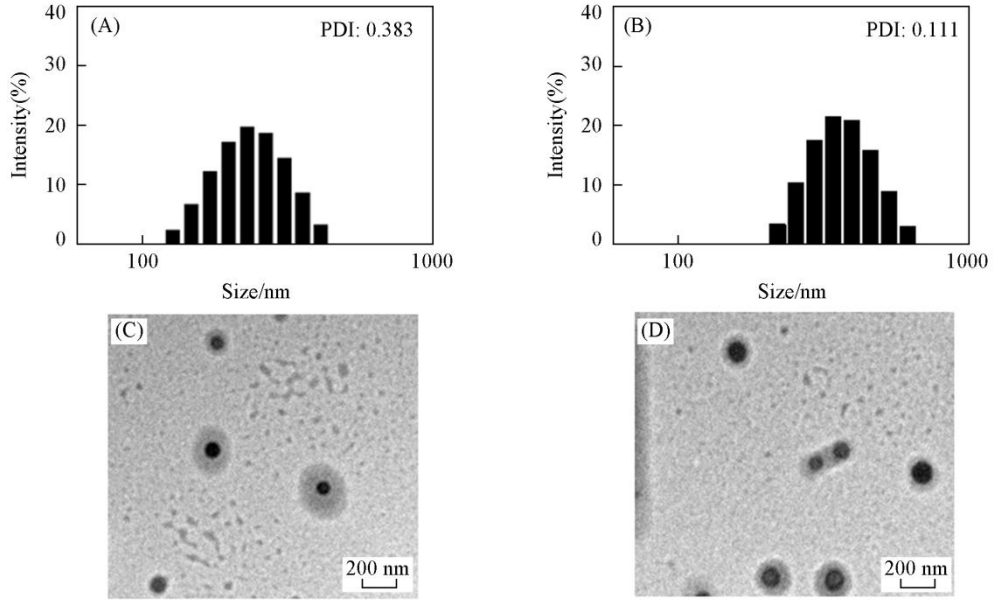

Fig.2 Particle size distribution of DNanoCapsule-A(A) and DNanoCapsule-B(B) determined by DLS, and TEM images of DNanoCapsule-A(C) and DNanoCapsule-B(D)

(PDI: 0.383) and 362.4 nm(PDI: 0.111), respectively, by DLS measurement. Further, the TEM images confirmed a spherical core-shell structure, comprising of a dark DOX particle core and a gray polymer shell, suggesting that the polymer layer was successfully coated on the surface of the DOX nanoparticles by *in-situ* polymerization[Fig. 2(C) and (D)].

3.2 *In vitro* Dissolution Rate of DNanoCapsules

The content of DOX in the DNanoCapsules was detected using UV spectrophotometry. The drug-loading capacities were estimated to be 32.6% and 35.8% for DNanoCapsule-A and DNanoCapsule-B, respectively. Further, to compare the pH-responsive DOX release behaviors of both DNanoCapsule-A and DNanoCapsule-B, various pH levels simulating the microenvironment of the endosomes/lysosomes of tumor cells(pH 5.0—6.0) and the blood or normal tissues(pH 7.4) were adopted. For DNanoCapsule-A, there are no significant differences of drug release in various pH levels, and the cumulative DOX release was only around 40% after 24 h incubation[Fig.3(A)]. Compared to DNanoCapsule-A, DNanoCapsule-B showed similar drug release behavior(41.8%) when the pH level was 7.4[Fig.3(B)]. However, the cumulative DOX release rates were significantly enhanced to 53.9% and 73.3% when the pH level decreased(pH 6.0 and 5.0)[Fig.3(B)], thus suggesting the pH-responsive drug release behaviors of DNanoCapsule-B.

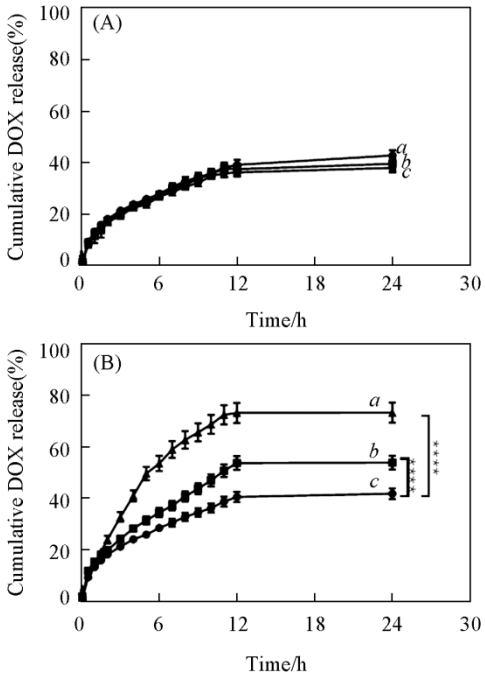

Fig.3 Cumulative DOX-release profiles of DNanoCapsule-A(A) and DNanoCapsule-B(B) in buffers of different pH values of 5.0(*a*), 6.0(*b*), and 7.4(*c*)

Data represent means±SD(n=3). **** $P < 0.0001$.

The results of the dissolution rate implied that the polymer layer of DNanoCapsule-B, constructed by a pH-sensitive GDA cross-linker, can prevent DOX leakage in blood circulation and normal tissues effectively, but enable DOX release in the acidic microenvironment of tumor and cancer cells. This may greatly improve the efficiency of anticancer drugs.

3.3 *In vitro* Cellular Uptake of DNanoCapsules

We used CLSM and FCM to investigate the *in vitro* cellular uptake of the DNanoCapsules in MCF-7 cells. As shown in Fig.4, the bright-red fluorescent signal of DOX was observed in the cells incubated with both DNanoCapsules-A and -B. Consistent with CLSM results, the cells incubated with both DNanoCapsules also exhibit significantly fluorescence intensity as compared to control sample(Fig.5). Both CLSM and FCM results demonstrated that the DNanoCapsules can be efficiently taken up by the cells.

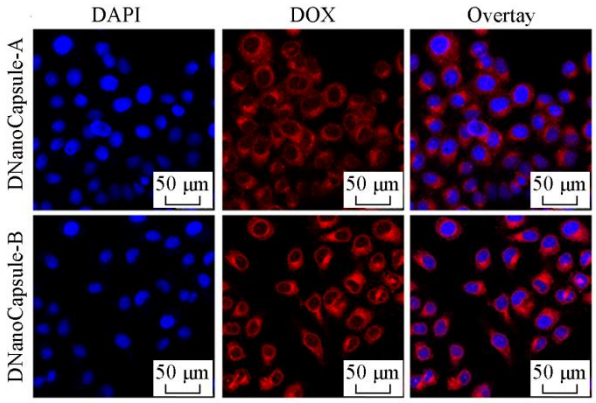

Fig.4 CLSM of MCF-7 cells after treatment with DNanoCapsule-A and DNanoCapsule-B

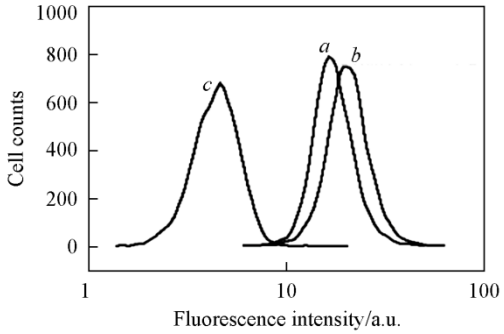

Fig.5 FCM of MCF-7 cells after treatment with DNanoCapsule-A(*a*), DNanoCapsule-B(*b*) and control(*c*)

We next studied the release capability of the DNanoCapsules. The late endosomes and lysosomes of MCF-7 cells after incubation with DNanoCapsule-B were stained by LysoTracker Green and imaged by CLSM. During the initial 4 h co-incubation, the overlaid yellow fluorescence in the endosomes and lysosomes suggests that a large number of DNanoCapsules were co-located with endosomes/lysosomes (Fig.6). Nevertheless, as the time extended to 24 h, an obvious separation of the red fluorescence of DOX and the green fluorescence of the endosomes/lysosomes was observed, indicating that the DNanoCapsules could escape from the endosomes/lysosomes and enter into the cytoplasm through the endocytosis[32].

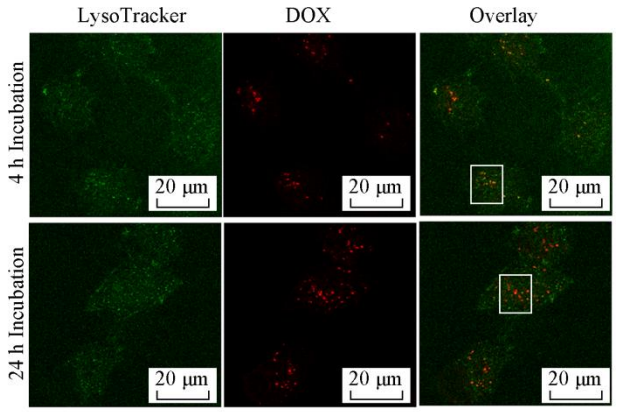

Fig.6 CLSM of LysoTracker green staining of MCF-7 cells after treatment with DNanoCapsule-B for 4 and 24 h

3.4 *In vitro* Cytotoxicity Assay of the DNanoCapsules

To evaluate the *in vitro* cytotoxicity of the DNanoCapsules, the cell viability was assessed using the MTT assay. Both HeLa and MCF-7 cancer cells were treated with free DOX, DNanoCapsule-A and DNanoCapsule-B at a series of DOX concentrations ranging from 3.3 μg/mL to 33.3 μg/mL for 24 h. In comparison to DNanoCapsule-A, DNanoCapsule-B exhibits a higher cytotoxicity with 25.8% and 24.7% living cells for HeLa and MCF-7 cells, respectively, at the highest DOX concentration of 33.3 μg/mL[Fig.7(A) and (B)]. To visually identify live and dead cells after treatment with the DNanoCapsules, the live-dead assay was adopted for staining live cells with green fluorescence(ethidium homodimer-1) and dead cells with red fluorescence(calcein-AM). As shown in Fig.8(A) and (B), free DOX treated groups exhibited the highest cell death ratio due to its small molecule structure resulted in high cellular uptake rate. Furthermore, the ratio of dead cells(red fluorescence) to live cells(green fluorescence) in the DNanoCapsule-B treated groups was enhanced as compared to the DNanoCapsule-A treated groups, indicating that the cytotoxicity of the DNanoCapsule-B was higher than the DNanoCapsule-A for both MCF-7 and HeLa cell-lines, which consistent with the MTT assay. Taken together, the enhanced cytotoxicity of DNanoCapsule-B was attributed to the accelerated DOX release rate, which was caused by the degradation of the polymer layer in the acidic microenvironment of cancer cells.

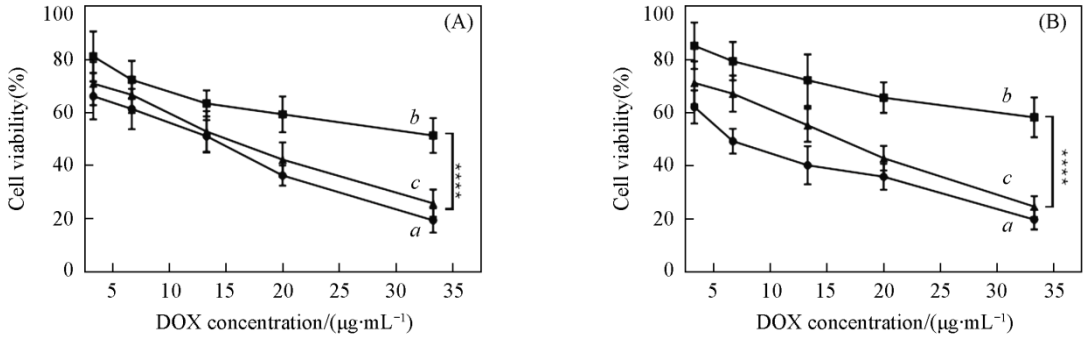

Fig.7 MTT assay of HeLa cells(A) and MCF-7 cells(B) after treatment with free DOX(*a*), DNanoCapsule-A(*b*) and DNanoCapsule-B(*c*)

Data represent means±SD(n=3). ****P < 0.0001.

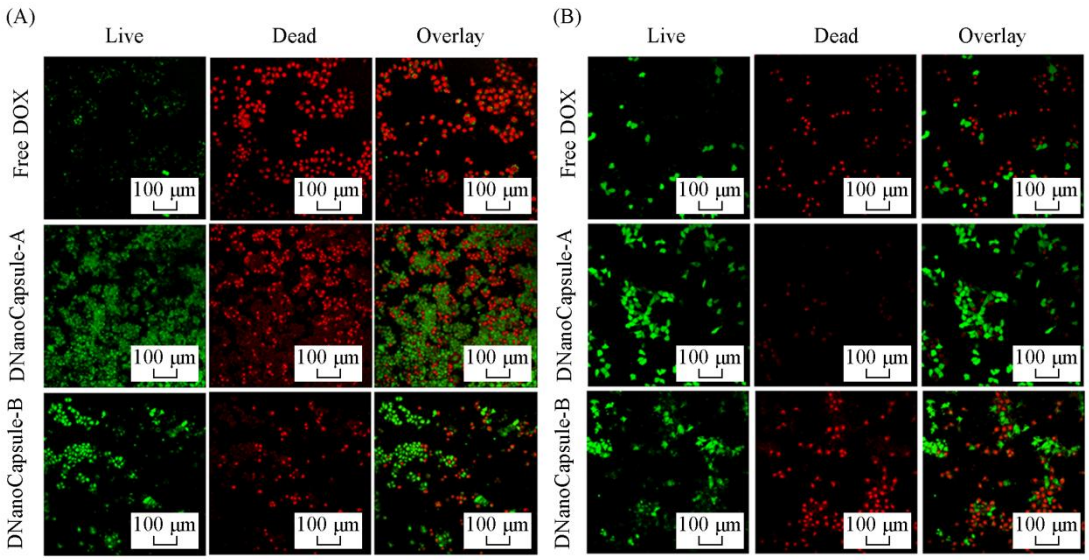

Fig.8 Live-dead staining(green=live, red=dead) of HeLa cells(A) and MCF-7 cells(B) after treatment with free DOX, DNanoCapsule-A, and DNanoCapsule-B

4 Conclusions

A novel DOX nanocapsule was developed by combining HGAP and *in-situ* polymerization technique through an amphiphilic polymerized surface ligand. The DOX nanocapsules exhibited a spherical structure with a drug particle core and polymer shell. The *in vitro* drug release studies showed that by introducing a pH-sensitive cross-linker, the nanocapsules exhibited rapid DOX release behavior under acidic conditions. Furthermore, the cellular uptake experiments demonstrated that DOX nanocapsules can be efficiently taken up by the cells *via* an endocytosis pathway. Finally, the effective cytotoxicity of the DOX nanocapsules was validated in both the HeLa and the MCF-7 cancer cell-lines. We believe that such a synthesis strategy of drug nanocapsules could be further adapted to design various stimuli-responsive drug formulations by regulating functional monomers and degradable cross-linkers for potentially treating diverse diseases.

References

[1] Kievit F. M., Zhang M. Q., *Advanced Materials*, **2011**, *23*(36), H217

[2] Cheng R., Meng F. H., Deng C., Klok H. A., Zhong Z.Y., *Biomaterials*, **2013**, *34*(14), 3647

[3] Sun Q. H., Radosz M., Shen Y. Q., *Journal of Controlled Release*, **2012**, *164*(2), 156

[4] Sun Q. H., Zhou Z. X., Qiu N., Shen Y. Q., *Advanced Materials*, **2017**, *29*(14), 1606628

[5] Doshi N., Samir M., *Advanced Functional Materials*, **2009**, *19*(24), 3843

[6] Wang Y., Wei G. Q., Zhang X. B., Xu F. N., Xiong X., Zhou S. B., *Advanced Materials*, **2017**, *29*(12), 1605357

[7] Ryu J. H., Chacko R. T., Jiwpanich S., Bickerton S., Babu R. P., Thayumanavan S., *Journal of the American Chemical Society*, **2010**, *132*(48), 17227

[8] Städler B., Price A. D., Zelikin. A. N., *Advanced Functional Materials*, **2010**, *21*(1), 14

[9] Hinton T. M., Monaghan P., Green D., Kooijmans S. A. A., Shi S., Breheney K., Tizard M., Nicolazzo J. A., Zelikin A. N., Ward K., *Acta Biomaterialia*, **2012**, *8*(9), 3251

[10] Wang Y. J., Yan Y., Cui J. W., Hosta-Rigau L., Heath J. K., Nice Edouard C., Caruso F., *Advanced Materials*, **2010**, *22*(38), 4293

[11] Guo Y. Q., Xu G. J., Yang X. T., Ruan K. P., Ma T. B., Zhang Q. Y., Gu J. W., Wu Y. L., Liu H., Guo Z. H., *Journal of Materials Chemistry C*, **2018**, *6*(12), 3004

[12] Wang Y. G., Wang Y. R., Hosono E., Wang K. X., Zhou H. S., *Angewandte Chemie International Edition*, **2008**, *47*(39), 7461

[13] Hu Z., Liu C. B., *Journal of Polymer Research*, **2012**, *20*(1), 39

[14] Jia X. Q., Wan L. Y., Du J. J., *Nano Research*, **2018**, *11*(10), 5028

[15] Chiou H., Li L., Hu T. T., Chan H. K., Chen J. F., Yun J., *International Journal of Pharmaceutics*, **2007**, *331*(1), 93

[16] Liu Y. P., Wu K., Wang J. X., Le Y., Zhang L. L., *Chemical Engineering Journal*, **2018**, *334*, 1766

[17] Hu T. T., Chiou H., Chan H. K., Chen J. F., Yun J., *Journal of Pharmaceutical Sciences*, **2008**, *97*(2), 944

[18] Zhang Z. L., Ji J. B., *Powder Technology*, **2017**, *305*, 546

[19] Hu Y. T., Wang J. X., Shen Z. G., Chen J. F., *Particuology*, **2008**, *6*(4), 22

[20] Mura S., Nicolas J., Couvreur P., *Nature Materials*, **2013**, *12*(11), 991

[21] Li Y., Li Y. H., Ji W. H., Lu Z. G., Liu L. Y., Shi Y. J., Ma G. H., Zhang X., *Journal of the American Chemical Society*, **2018**, *140*, 4164

[22] Zhang J. J., Li Y. X., Wang J. X., Qi S. P., Song X. Q., Tao C., Le Y., Wen N., Chen J. F., *RSC Advances*, **2017**, *7*, 53552

[23] Zhu L., Kate P., Torchilin V. P., *ACS Nano*, **2012**, *6*(4), 3491

[24] Sun C. Y., Liu Y., Du J. Z., Cao Z. T., Xu C. F., Wang J., *Angewandte Chemie International Edition*, **2015**, *55*(3), 1010

[25] Liang K., Such G. K., Johnston A. P. R., Zhu Z. Y., Ejima H., Richardson J. J., Cui J. W., Caruso F., *Advanced Materials*, **2013**, *26*(12), 1901

[26] Li B., Meng Z., Li Q. Q, Huang X. Y., Kang Z. Y., Dong H. J., Chen J. Y., Sun J., Dong Y. S., Li J., Jia X. S., Sessler J. L., Meng Q. B., Li C. J., *Chemical Science*, **2017**, *8*(6), 4458

[27] Huh K. M., Kang H. C., Lee Y. J., Bae Y. H., *Macromolecular Research*, **2012**, *20*(3), 224

[28] Li Y., Bui Q. N., Duy L. T. M., Yang H. Y., Lee D. S., *Biomacromolecules*, **2018**, *19*(6), 2062

[29] Yan M., Du J. J., Gu Z., Liang M., Hu Y. F., Zhang W. J., Priceman S., Wu L., Zhou Z. H., Liu Z., Segura T., Tang Y., Lu Y. F., *Nature Nanotechnology*, **2009**, *5*(1), 48

[30] Jiang G. Q., Liu C., Liu X. L., Zhang G. H., Yang M., Liu F. Q., *Macromolecular Materials and Engineering*, **2009**, *294*(12), 815

[31] Zhang J. J., Tokatlian T., Zhong J., Ng Quinn K. T., Patterson M., Lowry W. E., Carmichael S. T., Segura T., *Advanced Materials*, **2011**, *23*(43), 5098

[32] Jiang T. Y., Mo R., Bellotti A., Zhou J. P., Gu Z., *Advanced Functional Materials*, **2014**, *24*(16), 2295